DME/TACAN Interference and its Mitigation in L5/E5 Bands

Grace Xingxin Gao
Stanford University, CA, USA

BIOGRAPHY

Grace Xingxin Gao is a Ph.D. candidate under the guidance of Professor Per Enge in the Electrical Engineering Department at Stanford University. She received a B.S. in Mechanical Engineering in 2001 and her M.S. in Electrical Engineering in 2003, at Tsinghua University, Beijing, China. Her current research interests include GNSS signal and code structures, GNSS receiver architectures, and interference mitigation.

ABSTRACT

The Galileo E5a/E5b signals and the GPS L5 signal lie within the Aeronautical Radionavigation Services (ARNS) band. They suffer interference from the services in this frequency band, in particular, high power pulsed signals from Distance Measuring Equipment (DME) and Tactical Air Navigation (TACAN) systems. The pulsed interference degrades received Signal to Interference and Noise Ratio (SINR), lowers the acquisition sensitivity and even causes the tracking loops to diverge. To maintain system accuracy and integrity, interference mitigation is beneficial and necessary.

In this paper, the Stanford GNSS Monitor System (SGMS) is used to investigate the DME/TACAN signal environment at Stanford, CA, USA. The DME/TACAN beacons of six nearby airports, Woodside, SJC, SFO, Sausalito, OAK, Moffet, are observed. The TACAN signals are characterized by a 15 Hz sinusoidal envelope with north reference pulse code patterns and another 135 Hz modulation with reference pulse group patterns.

Current DME/TACAN interference techniques can be categorized as time-domain approach and frequency-domain approach. 'Pulse blanking' is the time-domain method. It zeroes out the portion where the amplitude of the complex I/Q signal exceeds a certain threshold level related to the noise. Pulse blanking is simple to implement, can be executed in real time without extra delay and only functions when the interference exists. However, when blanking the interference pulses, it also zeroes out the signals over that time slot. If the pulses are extremely dense in time, all received signals including both DME/TACAN pulses and GNSS signals will be blanked. The tracking will fail due to the unavailability of the signal. Moreover, because of the Gaussian pulse tailing effect, pulse blanking cannot completely suppress the interference.

'Notch filtering' mitigates the pulse interference in the frequency domain, where the DME/TACAN signals appear as narrow-band frequency tones. If the signal spectral density at certain frequencies is above the noise spectral density, these frequency components will be filtered out. Notch filtering can thoroughly suppress the DME/TACAN interference, including the central part of the Gaussian pulse and the tails. It also preserves the energy of the signal superposed with the interference pulses in the time domain. However, it not only filters interference, but also removes the signal energy at the DME/TACAN frequencies. Even during the time period when there are no DME/TACAN pulses, the E5 signal at these frequencies is still suppressed. If there are multiple DME/TACAN transponders nearby, the filter design will be complicated due to multiple notches in the filter.

'Hybrid blanking' exploits the advantages of both pulse blanking and notch filtering. In the time domain, if an interference pulse is detected, it triggers the notch filtering of a slice of 12 μsec data centered at the estimated pulse position. Filtering is only implemented when DME/TACAN pulses exist. It overcomes the disadvantage of regular notch filtering, which always filters out the corresponding frequency components of the signal even when there is no interference. For the slices of data that are covered by DME/TACAN pulses, hybrid blanking preserves most of the signal energy, and thus overcomes the disadvantage of time-domain pulse blanking. The filter design is simple, as there is a high chance of pulses from one certain transponder within the 12 μsec time window, thus there is only one notch in the fitler

To evaluate these three methods, signals from the GIOVE-A test satellite are collected. The interference-mitigated signals are acquired with a multi-signal all-in-view GNSS software receiver. The correlation peak to next peak ratio (CPPR) and the correlation peak to mean

peak ratio (CPPM) are chosen as the figures of merit for evaluation.

INTRODUCTION

Unlike their L1 and E6 counterparts, E5 and L5 signals at 1176.45 MHz and 1207.14 MHz are exposed to a unique electromagnetic environment created by existing aeronautical system pulsed emitters, especially Distance Measuring Equipment (DME) and Tactical Air Navigation (TACAN) systems. DME provides distance measurement between aircraft and a ground station. TACAN additionally provides azimuth information and is a military system. These navigation systems consist of an airborne interrogator and a ground-based transponder. DME and TACAN operate in four modes (X, Y, W and Z) between 960 MHz and 1215 MHz in an Aeronautical Radionavigation Services (ARNS) band [1]. The ARNS frequency allocation chart in Figure 1 illustrates its overlap with the E5 band. Only the X-mode replies in the 1151-1213 MHz frequency band, and is composed of pulse pairs with an inter-pulse interval of 12 μsec [2, 3]. The DME/TACAN interference degrades the signal-to-interference plus noise ratio (SINR), causes the tracking loops of receivers to fail to converge, and makes the E5 decoding process more difficult than decoding L1 and E6 codes. [4]

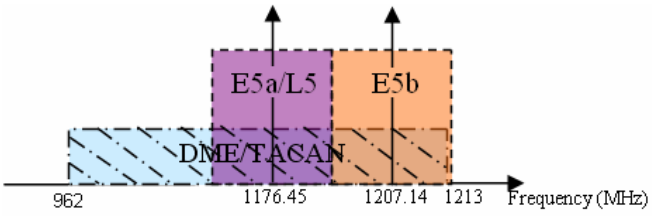

Figure 1. ARNS frequency allocation

The first section of this paper describes the DME/TACAN pulse structure, including DME pulse pairs and TACAN pulse amplitude modulation and reference pulse group patterns. The second section investigates the DME/TACAN interference environment at Stanford, CA, USA. Beacons of the nearby airports are identified; the DME pulse pairs and TACAN modulation and pulse groups are recognized. In the third and fourth sections, pulse blanking and notch filtering are introduced as current mitigation techniques. Hybrid blanking is proposed in the fifth section. Both pulse blanking and notch filtering have their advantages and disadvantages. Hybrid blanking combines the advantages of these techniques and avoids the disadvantages. Next, we compare these three techniques. We are able to apply them to real broadcast signals from the GIOVE-A and Compass M-1 satellites. We provide the PRN code generators information required for acquiring GIOVE-A and Compass M-1 signals [4, 9, 10]. But due to space limitations, we only show the results for the GIOVE-A E5a signals. The interference-mitigated signals are acquired with a GNSS software receiver. The correlation peak to next peak ratio (CPPR) and the correlation peak to mean peak ratio (CPPM) are used for evaluating the techniques.

DME/TACAN SIGNAL STRUCTURE

In the DME system, aircraft interrogators transmit pulses paired 12 μsec apart, each pulse lasting 3.5 μsec. The pulse-pair repetition rate ranges from 5 to 150 pulse pairs per second. The peak pulse power varies from 50 W to 2 kW. Paired pulses are used in order to reduce interference from other systems. [5]

Each pulse can be modeled as a Gaussian function. A pulse pair has the following expression [6], which is illustrated in Figure 2.

$$s_{pulse-pair}(t) = e^{-\frac{\alpha}{2}(t-\frac{\Delta t}{2})^2} + e^{-\frac{\alpha}{2}(t+\frac{\Delta t}{2})^2},$$

where $\alpha = 4.5 \times 10^{11}\ s^{-2}$

$\Delta t = 12 \times 10^{-6}$.

The constant α determines the pulse width, while Δt is the interpulse interval.

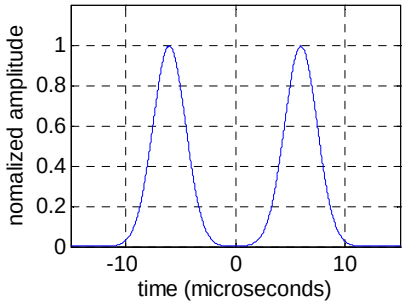

Figure 2. A simulated DME pulse pair

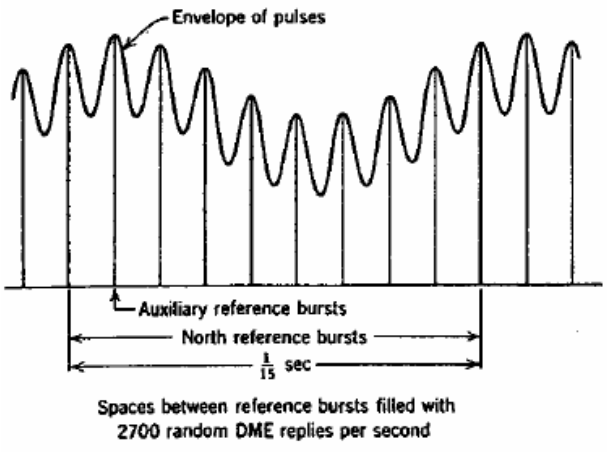

Figure 3. Transmitted TACAN Signal [5]

TACAN transponders transmit DME pulse pairs plus bearing reference pulses. A 15 Hz so-called north reference pulse code is emitted once per revolution, coincident with the maximum of the antenna pattern pointing east. This comprises 24 pulses, the spacing between pulses being alternately 12 and 18 µsec. Eight times per revolution, the 135 Hz reference pulse group of 12 pulses spaced 12 µ sec apart is emitted. (The ninth group coincides with the north pulse and is intentionally omitted.) The reference pulse groups have higher priority than normal constant-duty-cycle pulses. The overall transmitted pulse envelope is shown in Figure 3. The TACAN signals are amplitude modulated by a rotating antenna, reducing the effective sensitivity of the TACAN beacon about 3dB below that of an ordinary DME beacon. [5]

DME/TACAN SIGNAL ENVIRONMENT AT STANFORD

We use the Stanford GNSS Monitor System (SGMS) to investigate the DME/TACAN signal environment at Stanford, CA, USA. SGMS has a 1.8 m steerable parabolic dish antenna with an L-band feed. The antenna has approximately 7° beamwidth, and provides about 25 dB of gain over conventional patch antennas. We pointed the parabolic antenna to the GIOVE-A or Compass M-1 satellite and the DME/TACAN interference is received through the antenna side lobes. The motor of the antenna can be driven by satellite tracking software, so that the dish can automatically point to and track a specific satellite. The signal from the feed of the antenna goes through a low noise amplifier, a band pass filter, and is collected by an Agilent 89600 Vector Signal Analyzer (VSA). The VSA can down-convert the RF signal to baseband and save the data in computer-readable format.

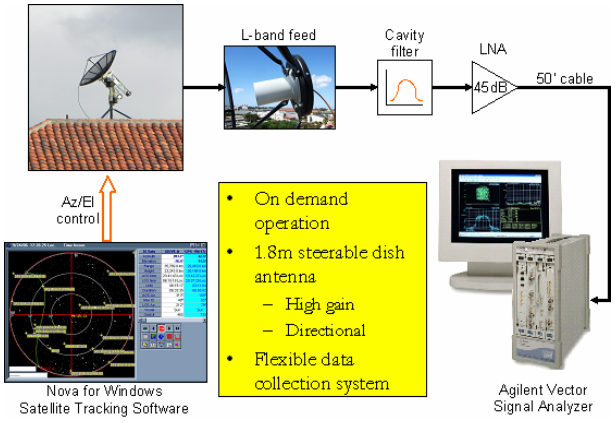

Figure 4. Block diagram of Stanford GNSS Monitoring System

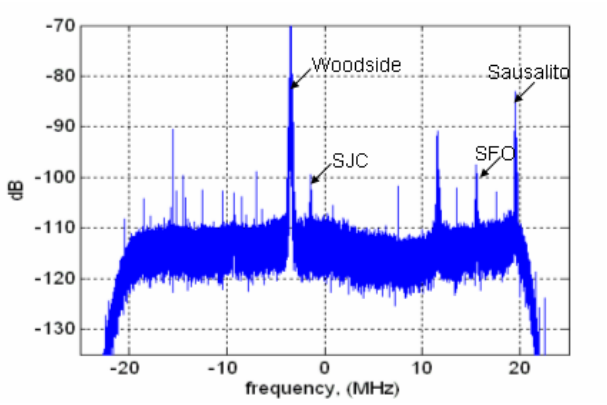

Figure 5. E5a power spectral density

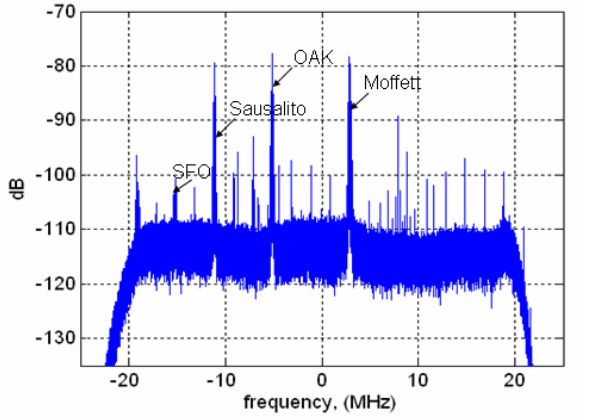

Figure 6. E5b power spectral density

Figures 5 and 6 show the power spectral density of the E5a and E5b frequency bands respectively. There are spikes in the frequency domain, corresponding to DME/TACAN beacons of nearby airports. The observed airports are Woodside, SJC, SFO, Sausalito, OAK, Moffett, as marked in Figures 5 and 6. The height of the spikes represents the received power of the corresponding DME/TACAN signals. The received power is a function of the distance from the airports to the observing location, the elevation of the airports and the transmitted power level. Table 1 shows the longitude, latitude, site elevation, antenna height and transmitter power of the DME/TACAN beacons around Stanford University. Among these beacons, Woodside is the closest. It also has a high elevation. This explains why the Woodside spike is highest in the spectrum.

Airport	Longitude	Latitude	Site elevation (ft)	Antenna height (ft)	Transmitter power (W)
Woodside	37.39278	-122.28194	2215	16	1173
Moffet	37.43222	-122.05694	4	N/A	1210
SFO	37.61944	-122.37389	13	26	1192
SJC	37.37472	-121.94472	56	33	1175
OAK	37.72583	-122.22333	10	N/A	1202
Sausalito	37.85528	-122.5225	1040	N/A	1196

Table 1. Airports near Stanford, CA, USA

The received E5a signal in the time domain is illustrated in Figure 7. The signal is amplitude modulated with envelope period of 66.67 msec, or equivalently at 15 Hz. This is generated by a parasitic element rotating around the antenna at 900 rpm. On top of the 15 Hz modulation, there is another 135 Hz sinusoidal modulation generated by nine other parasitic elements, also rotating at 900 rpm. Figure 8 shows the 135 Hz envelope with a period of 7.4 msec.

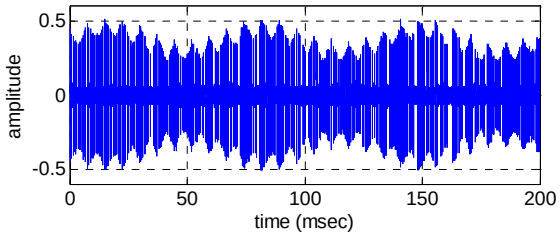

Figure 7. Received E5a signal, Inphase samples

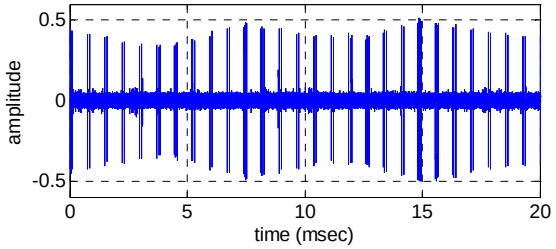

Figure 8. Received E5a signal, zooming in

If We zoom in further, We can see the pattern of the north reference pulse code, which consists of 24 pulses, being alternately 12 and 18 μsec apart, as shown in Figure 9. We also recognize the 135 Hz reference pulse group of 12 pulses with interpulse interval 12 μsec shown in Figure 10.

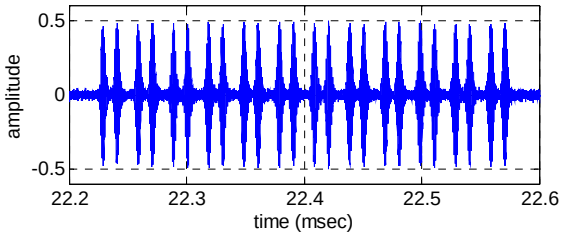

Figure 9. The 15 Hz north reference pulse group

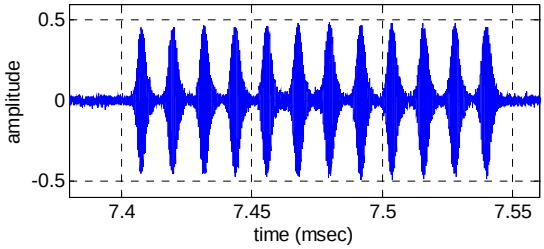

Figure 10. The 135 Hz reference pulse group

These pulse patterns identify the TACAN signal transmission. In addition to TACAN signals, there are also DME pulse pairs as shown in Figures 11 and 12. Figure 12 shows the Gaussian shape of the pulses. It also verifies the pulse width of 3.5 μsec and inter-pulse interval of 12 μsec. The observed signal matches the description in the previous section on DME/TACAN Signal Structure.

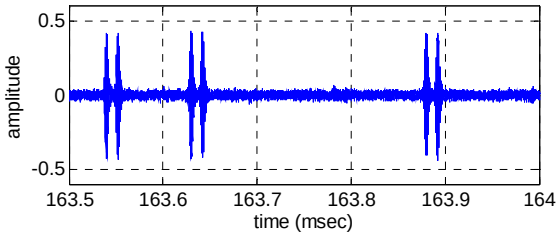

Figure 11. DME pulse pairs

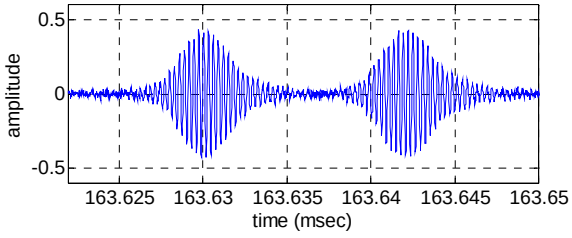

Figure 12. DME pulse pair, zooming in

PULSE BLANKING

The first interference mitigation technique we consider is pulse blanking, suggested by [1] and [2]. It blanks the signal whenever the norm of its amplitude exceeds a certain threshold level, as shown in Figure 13.

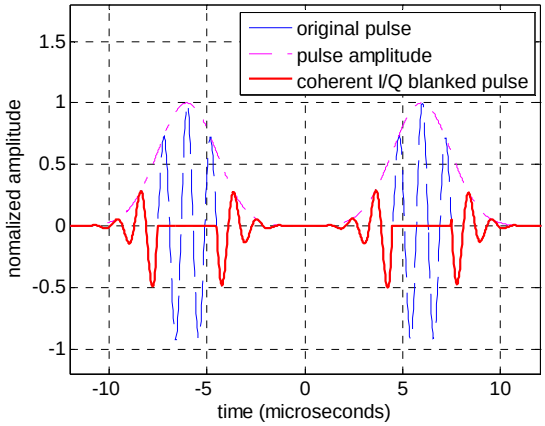

Figure 13. Pulse blanking

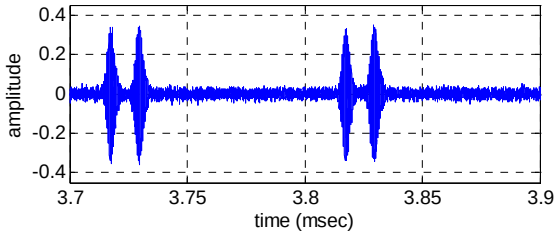

Figure 14. Time domain E5a signal before pulse blanking

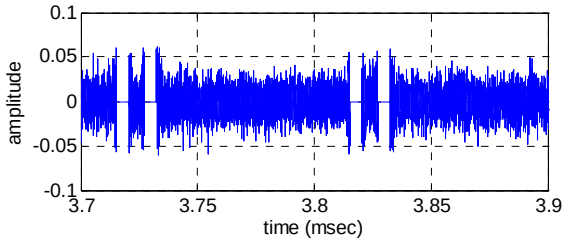

Figure 15. Time domain E5a signal after pulse blanking

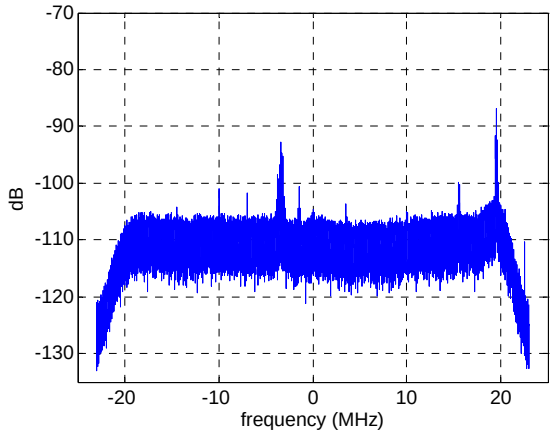

Figure 16. E5a power spectral density estimate, after pulse blanking

Figures 14 and 15 show the time domain E5a signal before and after pulse blanking. Figure 16 shows the power spectrum. In this example, pulse blanking mitigates 22 dB of DME/TACAN interference, reducing the spikes from -70 dB to -92dB. However, smaller spikes still exist at 17 dB above the noise floor.

Pulse blanking is effective and simple to implement but not thorough due to the bell shape of the DME/TACAN pulses. Their tails stretch below the noise floor, and thus cannot be removed by pulse blanking alone. In addition, when blanking the pulse interference, the E5 signal that coincides with the pulses is also blanked out. In this example, the DME/TACAN pulses occur 10 – 14% of the time. Pulse blanking would blank out 10 – 14% of the E5 signal, reducing its power. When pulses are extremely dense in time, pulse blanking will blank out a large portion of the GNSS signal or even the whole signal. It will make the signal unavailable and thus will fail tracking.

NOTCH FILTERING

The DME/TACAN signals have pulse characteristics not only in time domain, but also in frequency domain. In the frequency spectrum, the DME/TACAN signals appear as narrow-band frequency tones. Each frequency tone represents the signal from a nearby airport beacon. This motivates the mitigation of the DME/TACAN interference by notch filtering. Notch filtering removes the frequency components that exceed a certain level of the noise spectral density as shown in Figure 17.

Notch filtering has two merits. First, it can completely suppress the DME/TACAN interference, including both the central part and the tails of the Gaussian pulses. As the DME/TACAN signals only occur at certain frequencies, if the signal power at these frequency components is filtered out, DME/TACAN interference can be eliminated. Second, compared to time-domain pulse blanking, it preserves more of the energy of the E5 signal coincident with the interference pulses in time domain. Figure 18 shows the notch filtered data from the same time period as in Figure 15. The interference pulses disappear, while the E5 signal along with thermal noise remains.

However, notch filtering also has its drawbacks. Besides the interference, it also removes the E5 signal energy at the DME/TACAN frequencies. Since each nearby airport is mapped as a spike in the spectrum, a large number of airports in the surrounding area will result in many spikes in the spectrum. Filtering the frequency components of the spikes also filters out a large portion of the GNSS signal, even during time periods when there are no DME/TACAN pulses. Moreover, the design of the notch filter will become complicated as the number of nulls increases.

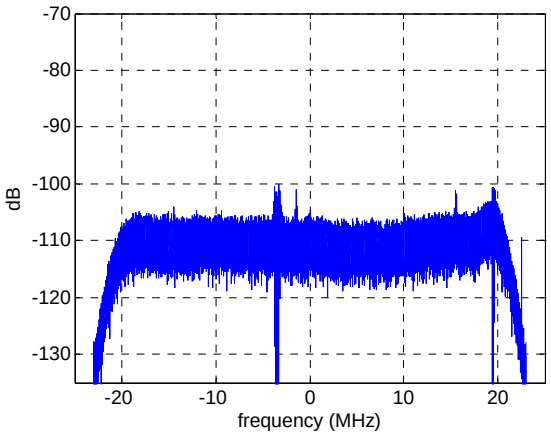

Figure 17. E5a power spectral density estimate, after notch filtering

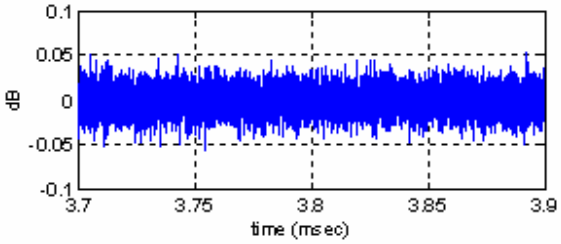

Figure 18. Time domain E5a signal, after notch filtering

HYBRID BLANKING

Pulse blanking and notch filtering both have advantages and disadvantages. Pulse blanking only functions when pulse interference occurs, but it can not eliminate the pulses completely. It also has the side effect of blanking the E5 signal coincident with the pulses in time. Notch filtering can suppress pulse interference thoroughly and preserve most of the energy of the E5 signal energy coincident with the pulses, but it degrades the signal power even when there are no DME/TACAN pulses. The notch filter design becomes difficult when there are several notches in the filter due to a large number of DME/TACAN transponders.

We propose another DME/TACAN interference mitigation technique, hybrid blanking, which combines the advantages of pulse blanking and notch filtering. The schematic of this technique is shown in Figure 19. The incoming signal is passed through a sliding window first. The next step is time-domain pulse detection. In time domain, if the amplitude of the incoming complex signal exceeds a certain level above the noise floor, a DME/TACAN pulse is detected. The pulse position is then estimated based on the center of mass of the signal in the segment. The pulse detection and the pulse center estimation trigger notch filtering. A 12 µsec segment of data centered at the estimated pulse position is converted into frequency domain and is fed into a notch filter. The choice of 12 µsec is due to the 12 µsec interpulse interval and the Gaussian tailing effect. The filtered piece of data is then converted back to the time domain and replaces the original portion as the output.

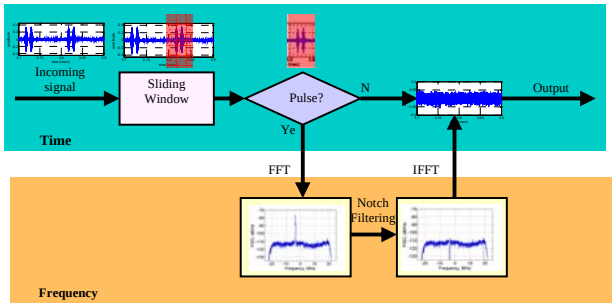

Figure 19. Hybrid blanking schematic

Figure 20 shows the selectivity of the three mitigation techniques in time and frequency domains. The horizontal axis shows the time duration of the pulses and the vertical axis shows the frequency extent. Pulse blanking is selective only in time and removes the GNSS signa in the region indicated by the vertical strips. This is most damaging when the pulse pairs are dense due to frequency aircraft landings. Notch filtering is selective only in frequency and removes the GNSS signal in the regions indicated by the horizontal stripes. This is most damaging when the pulses occur at many frequencies due to a large number of nearby airports. Hybrid blanking is both time and frequency selective. It only removes the GNSS signal in the regions indicated by the dots. This preserves more energy than pulse blanking or notch filtering alone. After hybrid blanking, the power spectral density of the E5a signal is shown in Figure 21 and the signal is shown in Figure 22.

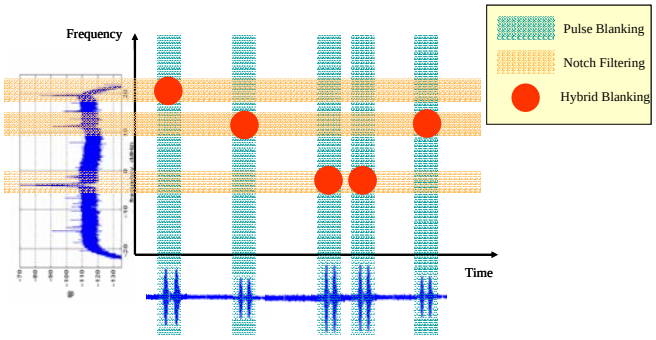

Figure 20. Selectivity of pulse blanking, notch filtering and hybrid blanking

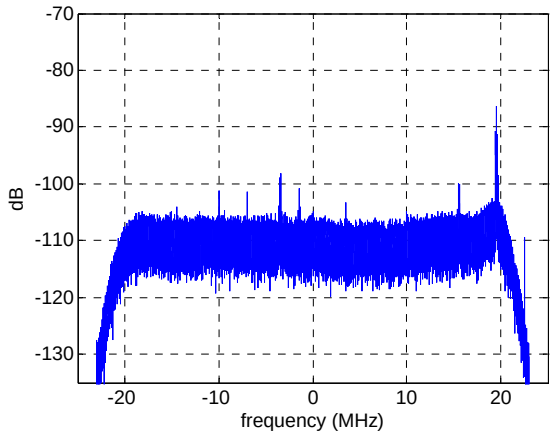

Figure 21. E5a power spectral density estimate, after hybrid blanking

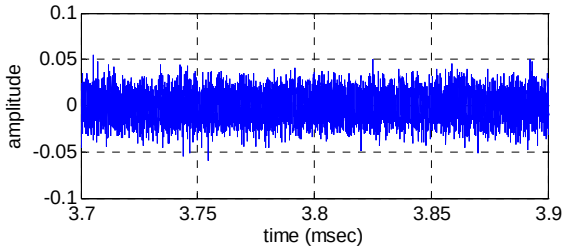

Figure 22. Time domain E5a signal, after hybrid blanking

ACQUISITION RESULTS

In the previous sections, we reviewed pulse blanking and notch filtering, and proposed hybrid filtering for mitigating DME/TACAN interference for GNSS receivers. We can evaluate these three methods using real signals from the Galileo GIOVE-A and Compass M-1 satellites. We condition the received signals by the three techniques and acquire them with a multi-signal all-in-view GNSS software receiver implemented in MATLAB™ [7, 8]. For reference, we include broadcast code information in tables 2 and 3 [4, 9, 10]. Due to space constraints, we only report the acquisition results fro the GIOVE-A E5a broadcast signal.

The real broadcast GNSS signals are acquired as a parallel code-phase search using FFT-based processing. We acquire 1 msec of data. The 3-D acquisition plots in Figure 21-28 show the normalized correlation function output as a function of code phase on one axis and carrier Doppler frequency on the other axis. We have two figures of merit to evaluate the mitigation techniques, CPPR and CPPM. These two figures reflect the post-processing signal to noise plus interference ratio.

Figure 23 and 24 show the acquisition plots of the Galileo E5a-I and E5a-Q channels without any mitigations. They look noisy. The CPPRs are only 6.77 dB and 5.93 dB respectively. These low peak ratios are due to the high DME/TACAN interference.

GIOVE-A broadcast codes		Type	Length	Period	Generated by
L1	L1-B	BOC (1,1)	4092	4msec	Two 13-stage LSRs
	L1-C	BOC (1,1)	8184	8msec	Two 13-stage LSRs
E6	E6-B	BPSK(5)	5115	1msec	Two 13-stage LSRs
	E6-C	BPSK(5)	10230	2msec	Two 14-stage LSRs
E5a	E5a-I	BPSK(10)	10230	1msec	Two 14-stage LSRs
	E5a-Q	BPSK(10)	10230	1msec	Two 14-stage LSRs
E5b	E5b-I	BPSK(10)	10230	1msec	Two 14-stage LSRs
	E5b-Q	BPSK(10)	10230	1msec	Two 14-stage LSRs

Table 2. GIOVE-A broadcast codes

Compass Broadcast		Type	Primary Code Period	Code Generators	Secondary Code Period
E2	I-channel	BPSK(2)	1 ms	11-stage Gold code	20 ms
E5b	I-channel	BPSK(2)	1 ms	11-stage Gold code	20 ms
E6	I-channel	BPSK(10)	1 ms	Two 13-stage Gold code	20 ms

Table 3. Compass M-1 broadcast codes

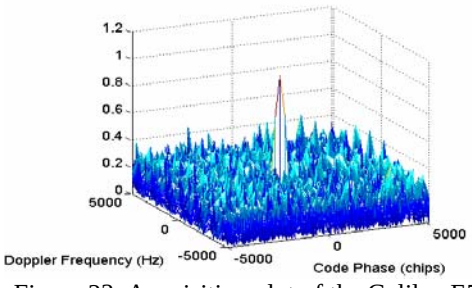

Figure 23. Acquisition plot of the Galileo E5a-I channel, raw data without DME/TACAN interference mitigation

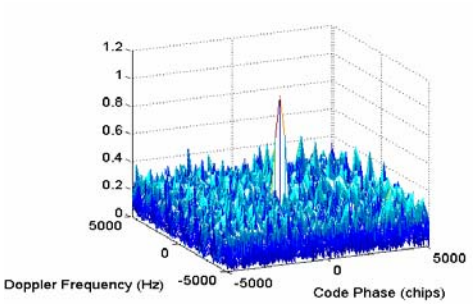

Figure 24. Acquisition plot of the Galileo E5a-Q channel, raw data without DME/TACAN interference mitigation

	CPPR (dB)	CPPM (dB)
E5a-I	6.77	16.90
E5a-Q	5.93	16.65

Table 4. Acquisition results of the E5a raw data

Next, we apply pulse blanking before sending the raw data into the acquisition module. Figures 25 and 26 show the acquisition results for E5a-I and E5a-Q channels. The integration time remains unchanged. Now we see less noisy plots. The CPPRs are increased from around 6 dB to 17 dB by the pulse blanking technique.

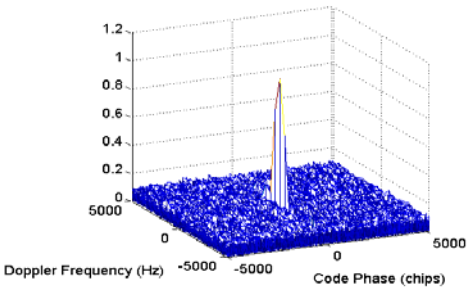

Figure 25. Acquisition plot of Galileo E5a-I channel, with pulse blanking

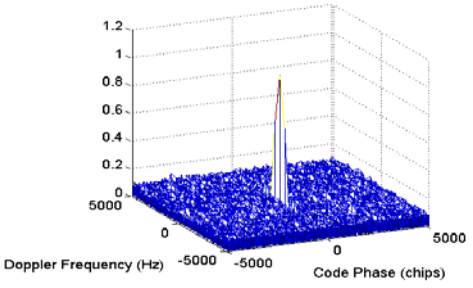

Figure 26. Acquisition plot of Galileo E5a-Q channel, with pulse blanking

	CPPR (dB)	CPPM (dB)
E5a-I	16.99	28.35
E5a-Q	16.78	28.37

Table 5. Acquisition results of the E5a pulse blanking

We also try applying notch filtering to the raw data. Figures 27 and 28 show the acquisition results for E5a-I and E5a-Q signals after notch filtering. The CPPRs and CPPMs are only slightly better than those of pulse blanking. The similar CPPRs and CPPMs of notch filtering and pulse blanking indicate that the loss due to notch filtering E5a signal when there are no interference pulses cancels out the gain from preserving the signal covered by these pulses.

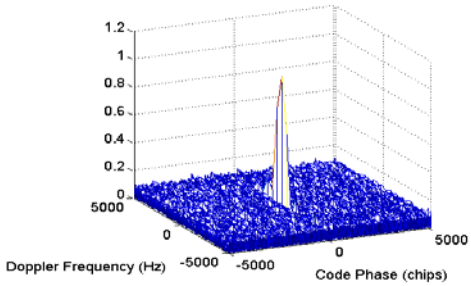

Figure 27. Acquisition plot of Galileo E5a-I channel, with notch filtering

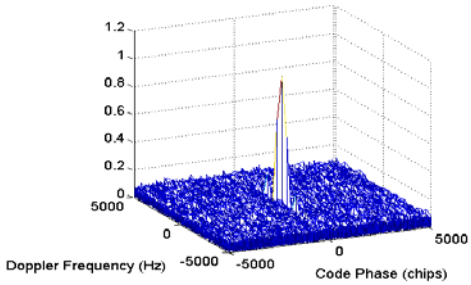

Figure 28. Acquisition plot of Galileo E5a-Q channel, with notch filtering

	CPPR (dB)	CPPM (dB)
E5a-I	17.50	28.93
E5a-Q	17.35	28.90

Table 6. Acquisition results of the E5a signal after notch filtering

We then evaluate the hybrid blanking technique. Figure 28 and 29 show the acquisition results for E5a-I and E5a-Q signals after hybrid blanking. The CPPRs and CPPMs are improved but only by less than 1 dB. This indicates that hybrid blanking has slightly better performance than pulse blanking or notch filtering. The benefit is marginal. Since the DME/TACAN pulses occur about 10% of the time in this example, the SINR improvement can only be up to 10%, or 1 dB. In busier DME/TACAN interference environments, the difference would be more significant. We intend to explore such environments in future work.

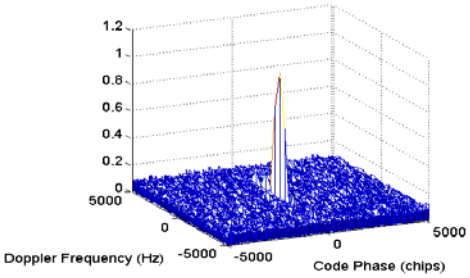

Figure 28. Acquisition plot of Galileo E5a-I channel, with hybrid blanking

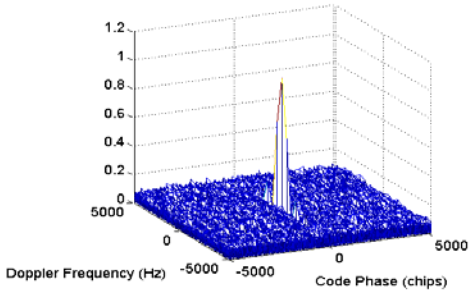

Figure 29. Acquisition plot of Galileo E5a-Q channel, with hybrid blanking

	CPPR (dB)	CPPM (dB)
E5a-I	17.70	29.15
E5a-Q	17.48	29.19

Table 7. Acquisition results of the E5a signal after hybrid blanking

CONCLUSION

The DME/TACAN interference environment at Stanford is investigated, hybrid blanking is proposed as a interference mitigation technique and the performance of pulse blanking, notch filtering and hybrid blanking are compared by acquiring real broadcast GNSS signals.

Hybrid blanking mitigates the interference in both time and frequency domain. It first detects the interference pulses in the time domain, and then filters the corresponding slices of data in the frequency domain. Hybrid blanking operates when the pulses occur, and preserves more GNSS signal energy compared to pulse blanking or notch filtering only. The notch filter used in the hybrid blanking technique is simpler than that in only notch filtering, as there is usually only one notch in the filter.

Hybrid blanking is also robust and works with no knowledge of the DME/TACAN environment. When there are very frequent aircraft landings, pulse blanking will fail by zeroing out all received signals, both interference and GNSS signals. When there are many airports or DME/TACAN transponders in the area, notch filtering will fail by blanking several the frequency components including those of the GNSS signals. Hybrid blanking is robust to the combination of these situation.

ACKNOWLEDGMENTS

The authors gratefully acknowledge the support of the Federal Aviation Administration under Cooperative Agreement 95-G-005. This paper contains the personal comments and beliefs of the authors, and does not necessarily represent the opinion of any other person or organization.

We would also like to thank Per Enge and Todd Walter for their guidance and supervision, and appreciate Ju-Yong Do for discussion, and Alan Chen and Sherman Lo for their help in data collection.

REFERENCES

[1]. T. Kim, J. Grabowski, ‘Validation of GPS L5 Coexistence with DME/TACAN and Link-16 System’, ION GNSS conference, Portland, OR, September 2003.

[2]. F. Bastide, E. Chatre, C. Macabiau, B. Roturier, ‘GPS L5 and Galileo E5a/E5b Signal-to-Noise Density Ratio Degradation Due to DME/TACAN signals: Simulation and Theoretical Derivation’, ION NTM Conference, San Diego, CA, January, 2004.

[3]. RTCA DO-292, ‘Assessment of Radio Frequency Interference Relevant to the GNSS L5/E5A Frequency Band’, July, 2004.

[4]. G. X. Gao, D. S. De Lorenzo, A. Chen, S. C. Lo, D. M. Akos, T. Walter and P. Enge, ‘Galileo GIOVE-A Broadcast E5 Codes and their Application to Acquisition and Tracking’, ION NTM Conference, San Diego, CA, January, 2007.

[5]. M. Kayton and W. R. Fried, ‘Avionics Navigation Systems, Second Edition’, John Wiley & Sons, Inc. 1997.

[6]. M. Monnerat, B. Lobert,, S. Journo and C. Bourga,, ‘Innovative GNSS2 Navigation Signal’, Proceedings of ION GPS Meeting, Salt Lake City, Utah, September, 2001.

[7]. D.S. De Lorenzo, J. Rife, P. Enge, and D.M. Akos, 2006, ‘Navigation Accuracy and Interference Rejection for an Adaptive GPS Antenna Array,’ Proc. ION GNSS 2006.

[8]. K. Borre, D.M. Akos, N. Bertelsen, P. Rinder, and S.H. Jensen, ‘A Software-Defined GPS and Galileo Receiver: A Single-Frequency Approach’, Birkhauser, 2006

[9]. G. X. Gao, J. Spilker, T. Walter, P. Enge, and A. R. Pratt, “Code Generation Scheme and Property Analysis of Broadcast Galileo L1 and E6 Signals,” ION GNSS 2006, Fort Worth, TX, Sep. 2006.

[10]. G. X. Gao, A. Chen, S. Lo, D. S. De Lorenzo and P. Enge, “GNSS over China, the Compass MEO Satellite Codes,” Inside GNSS Magazine, July-August 2007.